Extrusion behaviour of AZ91 Mg alloy produced by spark plasma sintering

P. Augusto de Oliveira Botelho[1], G. Straffelini*[1], C. Menapace[1], E. Mostaed[2] and M. Vedani[2]

Introduction

Mg alloys are of increasing interest in many applications because of their high specific strength and low density, which is comparable to that of polymers. Recently, Mg alloys have been proposed as biomaterials, since their corrosion products are considered harmless to human body when compared with other structural materials.[1–3] The necessary strength to support the cardiovascular vessel combined with controlled and non-toxic corrosion is reachable using Mg alloys.

Usually, Mg alloys are produced by casting technologies, and they can be submitted to hot working processes such as extrusion or forging. In order to avoid secondary processes, the powder metallurgy (PM) route is a possibility. This technology, however, is not largely used for Mg alloys because the Mg powders display a high reactivity to oxygen, and thus, they easily form oxide layers on their surfaces, which render difficult the sintering process. Within PM techniques, the spark plasma sintering (SPS) showed to be highly effective on breaking the oxide layers of the particle and giving good densification of sintered Mg alloys.[3,4] The possibility of producing cylindrical powder preforms made by AZ91 Mg alloy (with nominal chemical composition: 90Mg–9Al–1Zn–Mn, in wt-%) using SPS has been investigated in previous work.[3] The SPS cycle was optimised since the eutectic reaction between the Mg rich α phase and the β phase (with nominal composition $Mg_{17}Al_{12}$) produces a liquid at $\sim$440°C that proved to be unhelpful for SPS. A solubilisation treatment of the β phase is thus required before sintering. Furthermore, the possibility of hot extrusion of the cylindrical SPS preforms to produce rods with a diameter of 5 mm has also been verified.[5] It has been shown that hot extrusion at 350°C induced a dynamic recrystallisation (DRX) with a grain refinement of the starting microstructure.

The hot extrusion of Mg alloys has been widely investigated in order to increase the mechanical strength and modify the microstructure. DRX typically occurs in Mg alloys during hot deformation, if the temperature is sufficiently high, i.e. $>\sim$240°C. DRX reduces the grain size and the flow stress and thus increases the hot workability of the alloys.[6–8] This fact is of paramount importance when successive hot working processes have to be carried out, as is typical in Mg alloys. In fact, such alloys are characterised by quite a low room temperature ductility, and therefore, the possible cold working stage has to be reduced to a minimum.[9,10] The grain refinement by DRX of the AZ91 alloy has been recently investigated by Ravi Kumar *et al.*[7] The authors highlighted the correlation between the recrystallised grain size and the steady state flow stress. Ebrahimi *et al.*[11] showed that the fraction of DRX grains in the AZ91 alloy follows an Avrami equation, and that >90% DRX is attained after a strain of 0·6 already at 350°C. The authors also evinced some dependency of the DRX grain size and the total applied strain. All investigations presented in the literature are focused on Mg alloys produced by casting technologies.

This paper is part of a wider research project aimed at producing a fully bioabsorbable endovascular stent, made of Mg alloy. In the present study, we investigated the hot extrusion of SPS AZ91 powder preforms. The aim was to produce pre-extruded rods with fine grain

[1]Department of Industrial Engineering, University of Trento, 38123 Trento, Italy
[2]Department of Mechanical Engineering, Politecnico di Milano, 20156 Milan, Italy

*Corresponding author, email Giovanni.Straffelini@ing.unitn.it

and optimised hot extrudability in view of the successive production of small and thin wall tubes that are necessary for the realisation of the stents. Hot compression tests were also carried out to help in the characterisation of the extrusion behaviour, including an inverse determination of the lubrication regime.

Experimental

The cylindrical preforms for the present study were produced by SPS of AZ91 powders. The nominal chemical composition of the powders is 90Mg–9Al–1Zn (wt-%). They were produced by Ecka Granules GmbH and had a size <500 μm, with an average value of 200 μm.

The SPS process was carried in a Dr Sinter SPS 1050 with graphite die and punches. Cylindrical preforms with a diameter of 10 mm and height of 25 mm were produced. The cycle consisted of heating the sample up to 420°C at 50°C min^{-1}, holding it at this temperature for 1 h with the purpose of homogenise the material, heating to 470°C at 50°C min^{-1}, holding at this temperature for 10 min, and finally air cooling to room temperature. A pressure of 60 MPa was applied starting from a temperature of 350°C.

The direct extrusion tests were performed in a laboratory hot extrusion system installed in a 100 kN universal testing frame.[12] As is known, it is very difficult to exactly control the extrusion temperature of the billet, so that the temperature was monitored using a thermocouple inserted in the container, and making reference to a previous calibration of the temperature field in the extrusion device. The extrusion ratio, R, was 6·25, being the container diameter 10 mm and the diameter of the extruded rod 4 mm. Tests were performed at 330 and 380°C with the ram speed of 0·5 and 20 mm min^{-1}, which corresponded to strain rates of $1{\cdot}4\times10^{-3}$ and $5{\cdot}6\times10^{-2}$ respectively, evaluated according to the following equation:[13]

$$\dot{\varepsilon}=\frac{6VD_0\tan\alpha}{{D_0}^3-D^3}2\ln\left(\frac{D_0}{D}\right)$$

where $\dot{\varepsilon}$ is the strain rate, V is the ram speed in mm s^{-1}, α is the semiangle of the die, D_0 is the container diameter and D is the diameter of the extruded rod. Sample codes will be used in the present paper according to Table 1. In this table, the calculated values of the Zener–Hollomon parameter, Z, are also included (assuming 135 kJ mol^{-1} for the activation energy, Q[14,15]):

$$Z=\dot{\varepsilon}\cdot\exp(Q/R\cdot T)$$

To achieve information on the extrusion process, hot compression tests were also carried out using a Bahr 805A/D dilatometer. The tests were carried out with cylindrical samples with 2·5 mm diameter and 5 mm high, obtained by electrodischarge machining of the SPS preforms. The samples were cut in the same direction of pressing during sintering and were submitted to hot compression at 330 and 380°C at an average strain rate of 0·002 and 0·056 s^{-1} simulating the extrusion conditions at the speeds of 0·5 and 20 mm min^{-1} respectively.

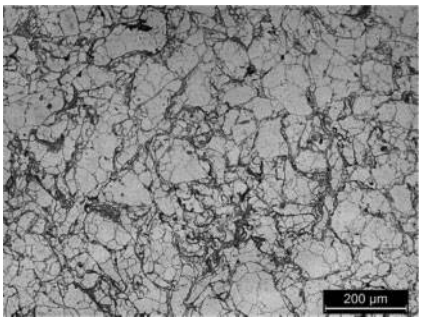

1 Microstructure of SPS sample

The microstructures of the SPS, hot extruded and hot compressed samples were observed using an optical microscope after etching with 2% Nital, and in a scanning electron microscope (SEM). X-ray diffraction (XRD) analysis was carried out to determine the present phases. Polished samples were exposed to Cu K_α radiation, and the amounts of the phases were determined with the Rietveld method.[16]

For the extruded materials, sections parallel to the extrusion direction were obtained for the observations. The grain size of the materials was measured using the planimetric (or Jeffries) procedure.[17] Microhardness tests were also carried out in different positions using a Vickers indenter and a load of 100 g.

Results and discussion

The microstructure of the SPS AZ91 alloy has been studied in detail in a previous work.[4] It was observed that SPS was able to induce almost complete densification, but it did not realise a complete welding between the original powders. Figure 1 shows an example of the microstructure. The original powder grains are decorated by grey areas that were found to be Mg oxides[4] that were already present on the powder surface, as shown by the energy dispersive X-ray spectroscopy (EDXS) analysis carried out on the surface of the powder (Fig. 2*a* and *b*). The presence of β phase was detected and measured by XRD (Fig. 2*c*). It turned out to be 17% in the powder and 6% in the SPS sample. Such a decrease after sintering was determined by the production cycle.[4] The average grain size of the SPS preforms was in the range 60–80 μm.

Figure 3 shows the microstructure of the materials after extrusion. In every case, DRX took place, leading to the formation of fine and equiaxed grains, in agreement with several investigations reported in the literature and, in particular, with the work of Ebrahimi *et al.*[11] However, the grain size is not uniform on the cross-section. The grains at the surface of the extruded

Table 1 Description of extrusion samples and its parameters

Sample name	Temperature/°C	Ram speed/mm min^{-1}	$\dot{\varepsilon}/s^{-1}$	Zener–Hollomon parameter/s^{-1}
330-05	330	0·5	$1{\cdot}4\times10^{-3}$	$6{\cdot}93\times10^{8}$
330-20	330	20	$5{\cdot}6\times10^{-2}$	$2{\cdot}77\times10^{10}$
380-05	380	0·5	$1{\cdot}4\times10^{-3}$	$8{\cdot}8\times10^{7}$
380-20	380	20	$5{\cdot}6\times10^{-2}$	$3{\cdot}5\times10^{9}$

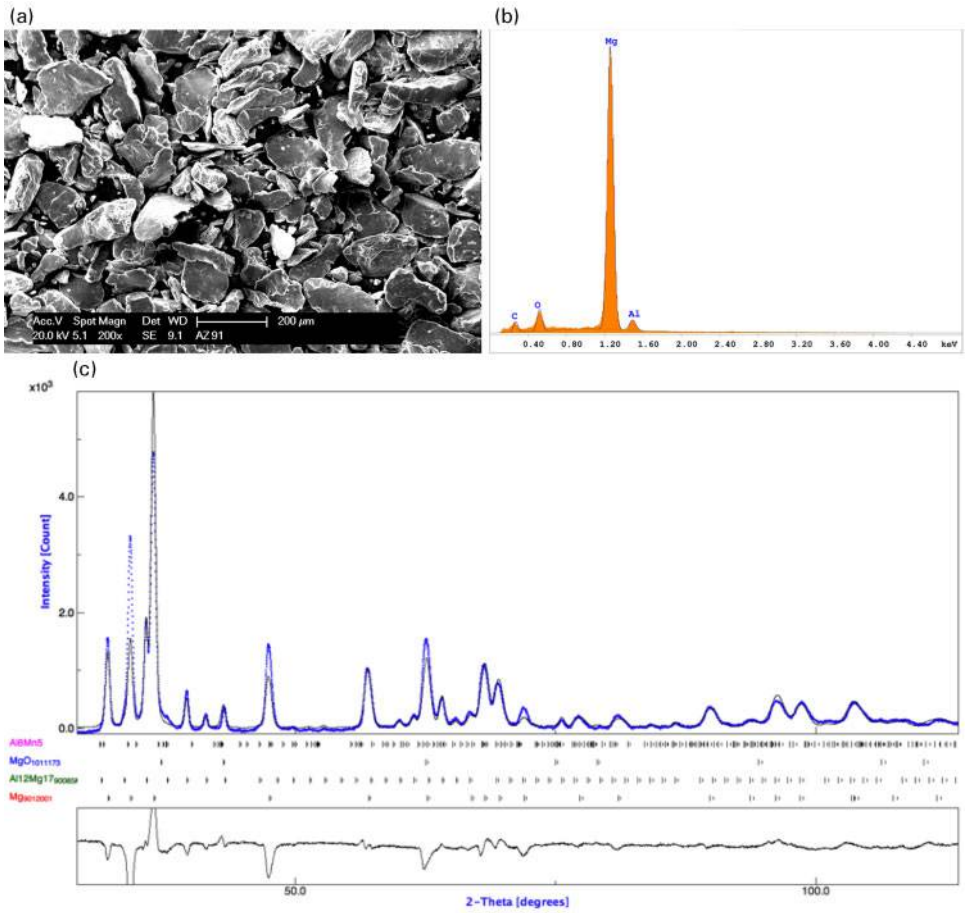

2 SEM (*a*), EDXS (*b*) and XRD (*c*) analysis of AZ91 powder (C peak in EDXS pattern is due to polymeric tape under powder)

bar are smaller than those at the centre of the rod. In Table 2 the average grain sizes of the materials under study at the surface and at the centre of the extruded rods are listed. In the same table, the results of the microhardness tests are also included. As expected, the microhardness decreases with increasing grain size. The observed difference in the recristallised grain size between the surface and the centre of the extruded rod may be explained by considering the greater surface plastic deformation promoted by contact with die surfaces during extrusion. Similar observations were also reported by Murai *et al.*[18] The increase in the strain and strain rate at the surface was also responsible for the formation of a subsurface crack in the material extruded at 330°C and at $5{\cdot}6 \times 10^{-2}$, i.e. with the highest value of Z. Figure 4 shows such a crack that might have formed by adiabatic shear banding.[19]

In order to analyse the influence of the extrusion parameters on the β phase dispersion, SEM and EDXS analyses were carried out on the metallographic samples (Fig. 5). Figure 5*a* shows the presence of three different phases. The first is the matrix, the second is a light grey phase identified as Al_8Mn_5 and the third one is the β phase (Fig. 5*b* and *c*). The β phase is an intermetallic with stoichiometric composition of $Mg_{17}Al_{12}$ formed in Mg–Al binary alloys. It has been shown that the same phase is also formed in ternary alloys containing Al and Zn (such as AZ91). In this case, the structure of the β phase is maintained with Zn atoms that replace some Al atoms. The reported stoichiometric composition is $Mg_{17}Al_{11{\cdot}5}Zn_{0{\cdot}5}$.[20] This explains the presence of Zn in the EDXS spectrum of β phase (Fig. 5*c*). Figure 5*a* shows that the intermetallic precipitates are quite uniform in the microstructure, and their size ranges between 1 and 3 μm. The amount of the present phases was obtained by the XRD patterns using the Rietveld method. The results are listed in Table 3. The MgO content is ~1% in every case, whereas the Al_8Mn_5 phase was not detected, showing that its content is clearly <1%. The amount of β phase is greater in the extruded samples than in the SPS sample, and it increases as extrusion temperature and strain rate are decreased. This can be explained by considering the Mg–Al phase diagram, which shows that at temperatures exceeding 380°C the β phase is dissolved into the Mg matrix, whereas at 330°C, it may precipitate in the microstructure. The minimisation of the β phase content is quite important from a technological point of view, since such a phase increases the brittleness of the alloys and decreases their corrosion resistance.[6,21]

Figure 6 shows the hot compression curves recorded at 330 and 380°C and at an average strain that simulate the extrusion conditions at the speeds of 0·5 and 20 mm min^{-1} (the curves are therefore indicated with 330-05, 330-30, 380-05 and 380-20). In every case, at the beginning, there is a rapid increase in the stress due to workhardening, which is given by the accumulation of dislocations. Quite soon, however, the flow stress reaches a peak value and then decreases. Such a decrease is commonly attributed to the occurrence of DRX,[7] and this

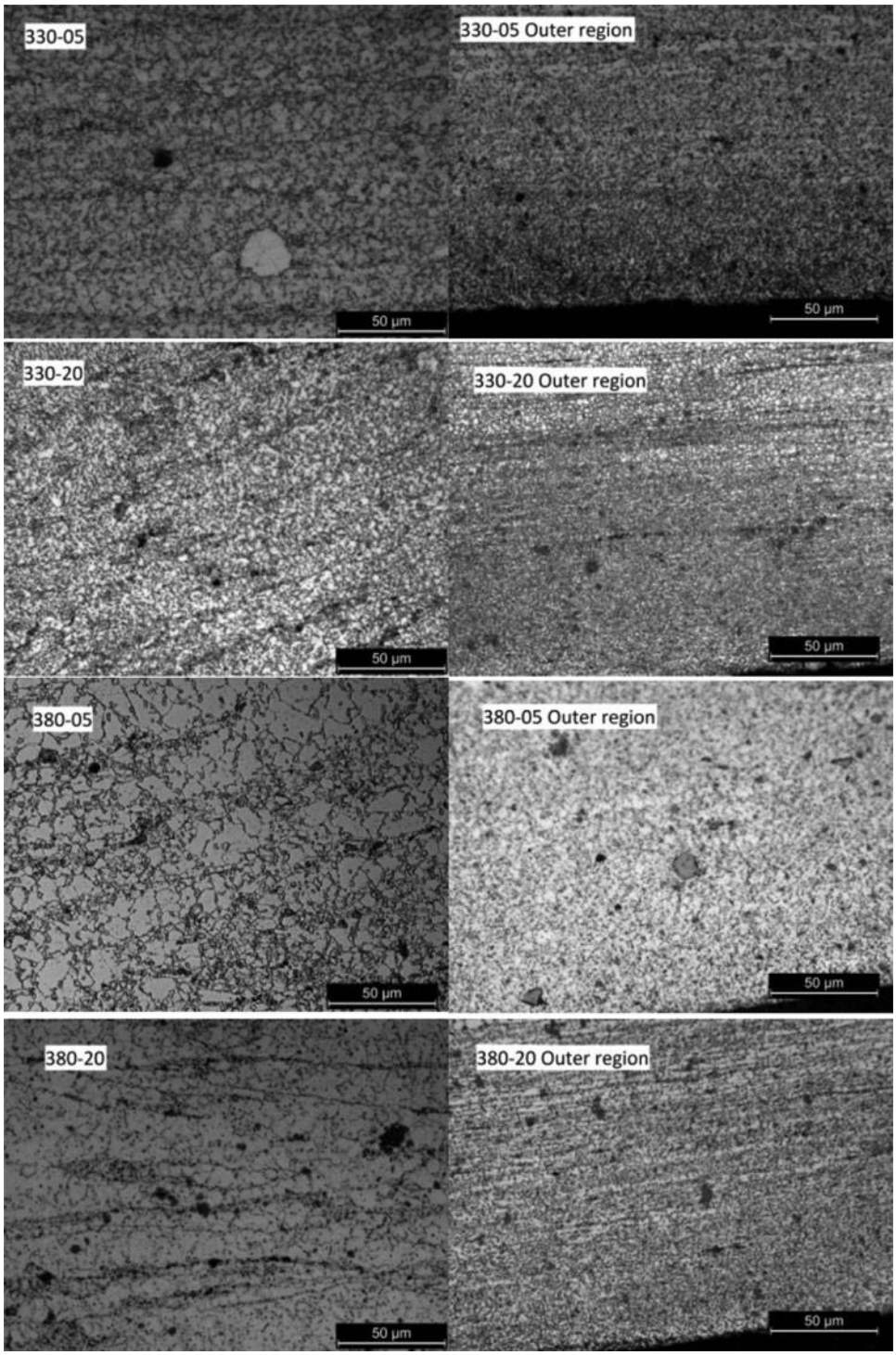

3 Grain size after extrusion in inner and outer regions

is actually in agreement with our observations, as shown by the microstructures in Fig. 7 and with the microstructural evolution recorded after extrusion. The DRX grain sizes after hot compression appear somewhat larger than those obtained after extrusion. This result can be explained by considering the experimental observations

Table 2 Measured grain sizes and microhardness values

Sample	Average grain size at centre/10^3 grains mm^{-2}	Average grain size at the surface/10^3 grains mm^{-2}	Microhardness at centre/HV100	Microhardness at surface/HV100
330-05	50	140	103	118·5
330-20	80	560	112	127
380-05	4	25	95	98
380-20	20	80	98	105

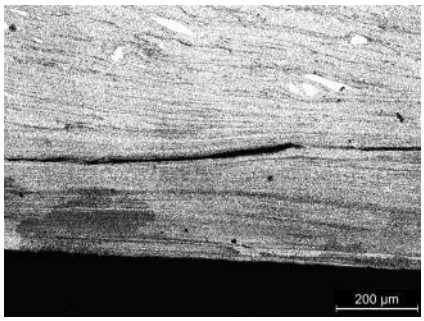

4 Shear crack in subsurface region of sample 380-20

reported by Ebrahimi *et al.*,[11] where DRX grain size is shown to decrease after large strains after having reached a peak value. We could thus say that after extrusion, the applied strains were larger than after the hot compression, then justifying the smaller DRX grain sizes.

The peak stresses, σ_e, measured from the graphs in Fig. 6, are listed in Table 4. As expected, they decrease with temperature and increase with strain rate. During the extrusion tests, the applied loads were recorded. They were found to increase when the samples were entering the die, and then to reach a maximum value when the die was completely filled. The recorded maximum extrusion loads (F_{max}) are also listed in Table 4. It is seen that they are proportional to the σ_e values obtained from the compression tests.

We therefore used the data listed in Table 4 to get an approximate evaluation of the average friction coefficient, μ, during hot extrusion. Since μ is defined as a ratio of forces, it cannot be measured directly and an inverse approach should be adopted.[22] To achieve this task, simple mechanical relations for extrusion were used, considering in particular that the maximum extrusion force, F_{max}, may be expressed by the sum of the force for plastic deformation and the friction force between the container and the billet. F_{max} is thus given by $p_{ext}\,A_o$, where p_{ext} is the total extrusion pressure and A_o is the initial cross-section of the billet (A_o=78·5 mm^2). p_{ext} is given by[13]

$$p_{ext} = p_0\left(1+\frac{4\,\mu L}{D_0}\right)$$

where p_o is the pressure for plastic deformation, μ is the average friction coefficient relevant to the magnesium/steel interface, L is the length of the billet in the container (25 mm) and D_o is the initial diameter of the billet (10 mm). The pressure p_o is related to the effective flow stress through the following relation:[13]

$$p_0 = \sigma_e(a + b\cdot\ln R)$$

where a and b are constants that can be assumed to be 1·06 and 1·55.[13] By using the peak values listed in Table 4 for

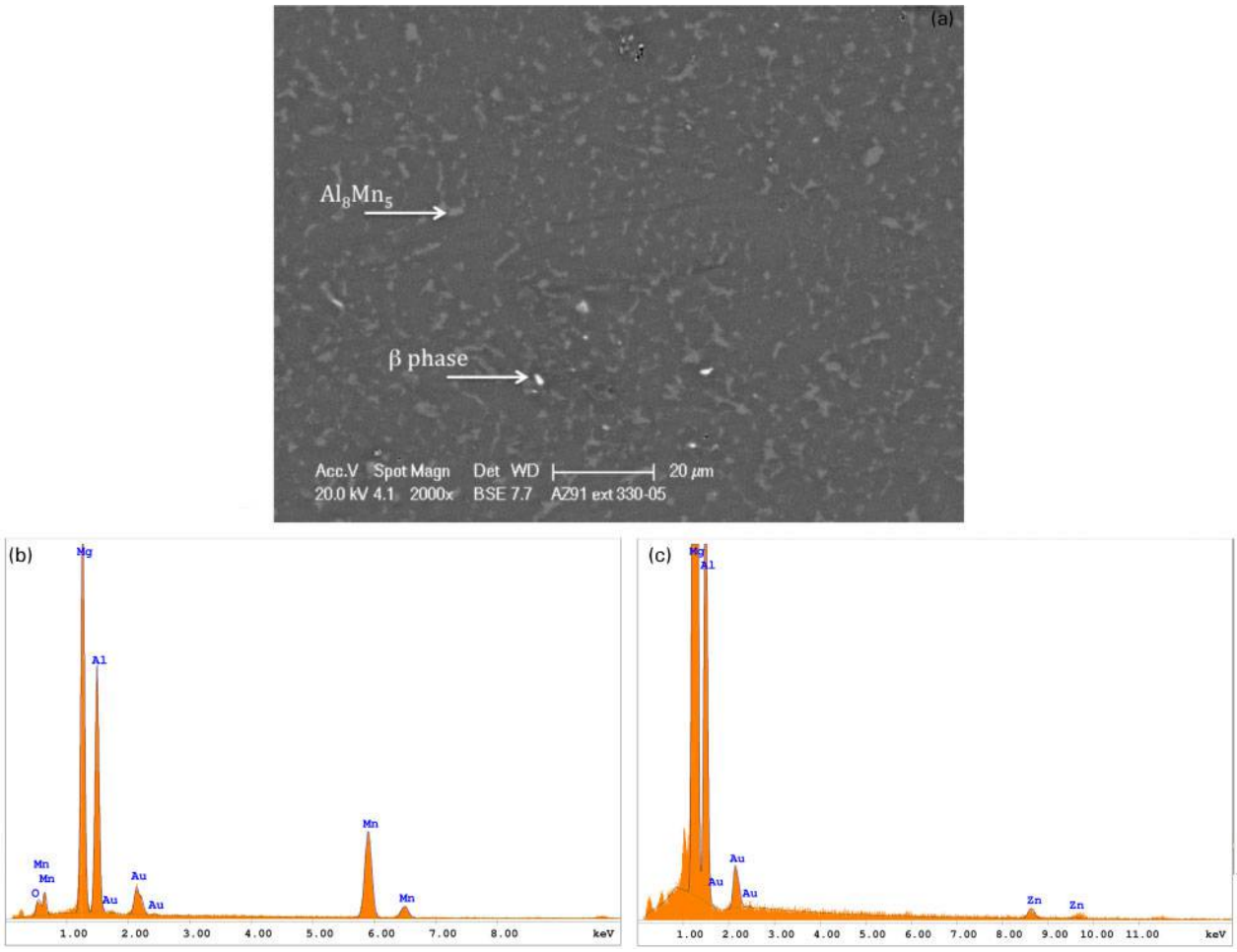

5 *a* SEM image on BSE mode of sample 330-05, showing β phase and Al_8Mn_5 intermetallic; *b* EDXS pattern of Al_8Mn_5; *c* EDXS pattern of β phase

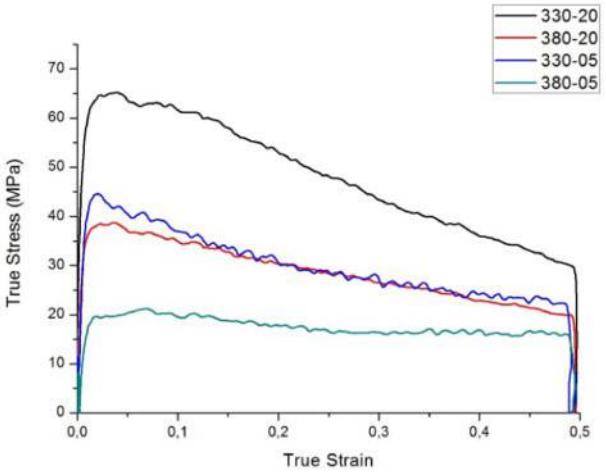

6 Hot compression curves of SPS samples

the estimation of σ_e and the maximum extrusion force also listed in Table 4, the average friction coefficients may be estimated, and they are listed in Table 4. In general, for the magnesium/steel interface, a friction coefficient ~0·3 is considered.[23] The data in Table 4 show that at 330°C, the used lubricant is able to induce a better lubrication regime, since μ is ~0·2, i.e. typical of a boundary lubrication condition.[24] As the extrusion temperature is increased to 380°, however, the average friction coefficient increases to 0·4–0·56, i.e. it becomes greater than the reference value. For the employed lubricant, an upper limit of 400°C for the temperature is suggested. Since the temperature on the die is not constant, in some points, the temperature can reach values higher than 400°C, being harmful for the lubricant performance. For the successive production of thin wall tubes, extrusions with higher values of the extrusion ratio will be carried out. The present results therefore suggest the opportunity of using a lubricant with an improved temperature resistance, such as a molybdenum disulphide paste, for extrusions at 380°C.

Table 4 Peak flow stress during hot compression, maximum extrusion load, and estimated friction coefficient during extrusion

Sample	σ_e/MPa	F_{max}/kN	μ calculated
330-05	45	37	0·20
330-20	65	54	0·20
380-05	20	35	0·44
380-20	37	50	0·56

Conclusions

The AZ91 Mg alloy was produced by SPS using an optimised cycle. The cylindrical specimens were then submitted to hot extrusion to produce rods with a diameter of 5 mm (R=6·25). The tests were carried out at 330 and 380°C, and a ram speed of 0·5 and 20 mm min^{-1}. In order to achieve further information on the deformation behaviour of the alloy and the friction regime during extrusion, hot compression tests were also carried out using small cylindrical specimens, at conditions very close to the extrusion tests.

The main results can be summarised as follows:

- The hot extrusion process produced a consolidation of the material because of DRX, which was accompanied by a noticeable grain refinement, from 60–80 μm after SPS down to 4–8 μm for the rods extruded at 20 mm min^{-1}.
- The alloy extruded at 330°C (lower temperature here investigated) and 20 mm min^{-1} (higher extrusion speed here investigated) contained some subsurface cracks formed by intense shearing. The other extruded alloys were found to be free from defects like cracks.
- As expected, the extruded alloys contained some residual β phase. The precipitates are ~1–3 μm in size, and they are uniformly distributed in the matrix. Its presence was found to be minimised after extrusion at 380°C (the measured amount was 10%).
- On the bases of the hot extrusion results, the optimal conditions were found 380°C and 20 mm min^{-1}.

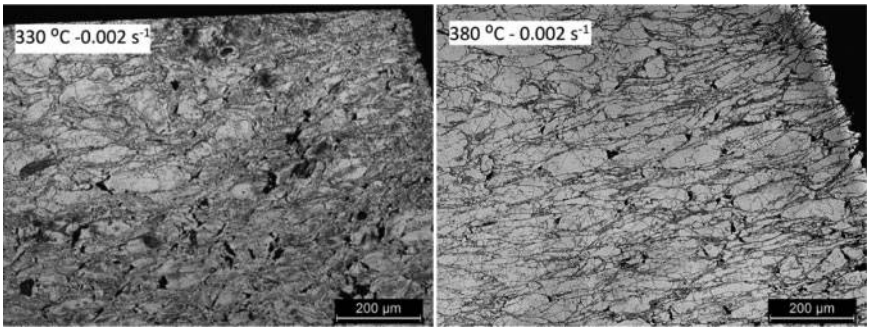

7 Microstructure after hot compression at different temperatures and at strain rate of 0·002 s^{-1}

Table 3 Phase content in materials under investigation

	AZ91 powder	AZ91 SPS	330-05	330-20	380-05	380-20
Mg Matrix	82%	93%	86%	88%	89%	89%
MgO	1%	1%	1%	1%	1%	1%
β Phase	17%	6%	13%	11%	10%	10%
Al_8Mn_5	Not detected	Not detected	Not detected	Not detected	Not detected	Not detected

- During hot compression testing, the SPS materials showed a typical behaviour characterised by initial strain hardening up to a peak value, followed by softening, which was attributed to the occurrence of DRX.
- An inverse evaluation of the average friction coefficient during extrusion allowed us to obtain that at 380°C/20 mm min^{-1} (the optimal conditions), lubrication was not particularly effective. It is therefore suggested to use a lubricant with an improved temperature resistance, such as a molibdenum disulphate paste, for future extrusions with higher extrusion ratios.
- The obtained results are promising in view of the successive steps necessary for producing thin wall tubes and then biodegradable stents, even if the corrosion behaviour has to be investigated to highlight the role of the remaining β phase in the microstructure.

Acknowledgement

The authors gratefully acknowledge the support from Fondazione Cassa di Risparmio di Trento e Rovereto (Trento, Italy).

References

1. F. Witte: *Acta Biomater.*, 2010, **6**, 1680–1692.
2. Q. Ge, D. Dellasega, A. Demir and M. Vedani: *Acta Biomater.*, 2013, 1–7.
3. G. Straffelini, A. P. Nogueira, P. Muterlle and C. Menapace: *Mater. Sci. Technol.*, 2011, **27**, 1582–1587.
4. W. N. A. W. Muhammad, Z. Sajuri, Y. Mutoh and Y. Miyashita: *J. Alloys Compd*, 2011, **509**, 6021–6029.
5. G. Straffelini, L. Dione da Costa, C. Menapace, C. Zanella and J. M. Torralba: *Powder Metall.*, 2013, **56**, 405–410.
6. S. W. Xu, N. Matsumoto, S. Kamado, T. Honma and Y. Kojima: *Mater. Sci. Eng. A*, 2009, **A523**, 47–52.
7. N. Ravi Kumar, J. Blandin, C. Desrayaud, F. Montheillet and M. Suéry: *Mater. Sci. Eng. A*, 2003, **A359**, 150–157.
8. Y. Uematsu *et al.*: *Mater. Sci. Eng. A*, 2006, **A434**, 131–140.
9. K. Yoshida and A. Koiwa: Proceedings of the ASME 2011 International Manufacturing Science and Engineering Conference (MSEC2011), Corvallis, Oregon, June 13–17, 2011, ASME, New York, 1–5.
10. G. Fang *et al.*: *Mater. Sci. Eng. C*, 2013, **C33**, 3481–3488.
11. G. R. Ebrahimi *et al.*: *Trans. Nonferrous Met. Soc. China*, 2012, **22**, 2066–2071.
12. Q. Ge, M. Vedani and G. Vimercati: *Mater. Manuf. Processes*, 2012, **27**, (2).
13. G. E. Dieter: 'Mechanical metallurgy, SI metric edition'; 1988, London, McGraw-Hill.
14. S. S. Vagarali and T. G. Langdon: *Acta Metall.*, 1974, **22**, 779–788.
15. H. Kim and W. Kim: *Mater. Sci. Eng. A*, 2004, **A385**, 300–308.
16. 'The elaboration of the XRD-spectra by the Rietveld method has been carried out using the program 'Maud' developed by L. Lutterotti', http://www.ing.unitn/.
17. ASTM Standard E112, 2013, 'Standard test methods for determining average grain size', ASTM International, West Conshohocken, PA, 2003, www.astm.org.
18. T. Murai, S. Matsuoka, S. Miyamoto and Y. Oki: *J. Mater. Process. Technol.*, 2003, **141**, 207–212.
19. Y. Chen, Q. Wang, J. Peng, C. Zhai and W. Ding: *J. Mater. Process. Technol.*, 2007, **182**, 281–285.
20. K. Braszczyńska-malik: 'Precipitates of gamma-Mg17Al12 phase in Mg–Al alloys, magnesium alloys—design, processing and properties', (ed. F. Czerwinski); 2011, Vienna, InTech.
21. G. Song, L. Bowles and D. H. StJohn: *Mater. Sci. Eng. A*, 2004, **A366**, 74–86.
22. J. G. Lenard: 'Metal forming science and practice'; 2002, Oxford, Elsevier.
23. R. Y. Lapovok, M. Barnett and C. H. Davies: *J. Mater. Process. Technol.*, 2004, **146**, 408–414.
24. I. M. Hutchings: 'Tribology: Friction and wear of engineering materials'; 1992, London, Edward Arnold.